IEEE Access
Multidisciplinary | Rapid Review | Open Access Journal

Received August 9, 2019, accepted September 11, 2019, date of publication September 18, 2019, date of current version October 4, 2019.

Digital Object Identifier 10.1109/ACCESS.2019.2942168

An Improved Radon-Fourier Transform Coherent Integration Method

YONGKUN SONG[1,2], TIAN JIN[1,2], (Member, IEEE), YONGPING SONG[3], AND YANSONG ZHANG[1]

[1]School of Electronic Science, National University of Defense Technology, Changsha 410073, China
[2]Science and Technology on Near-Surface Detection Laboratory, Wuxi 214035, China
[3]Air Force Early Warning Academy, Wuhan 430014, China

Corresponding author: Tian Jin (tianjin@nudt.edu.cn)

This work was supported in part by the Science and Technology on Near-Surface Detection Laboratory Foundation of China under Grant 614241408021810, and in part by the National Natural Science Foundation of China under Grant 61971430.

ABSTRACT Radar plays an increasingly important role in target detection because of its all-weather detection capability. Furthermore, to detect weak and flexible target, effectively coherent integration method is required in radar signal processing to enhance the target signal intensity. Based on the Radon-Fourier transform (RFT) algorithm, which is widely used to solve the problem of weak target detection, range migration and Doppler ambiguity in low signal-to-noise ratio (SNR) environment, an improved multiple pulse repetition intervals (PRIs) RFT (MRFT) coherent integration method is presented in this paper. The method adopts the Linear frequency modulated (LFM) signal with three different PRIs as the transmitted signal, then combines with the RFT outputs of three RPIs to enhance the target energy and suppress the blind speed side lobe (BSSL) caused by RFT. Meanwhile, the design rules and constraints of this method are also discussed in detail. The experiments with simulation data and real measured data are provided to demonstrate that the designed method can get better BSSL suppression capability and higher detection rate than conventional methods.

INDEX TERMS Coherent integration, multiple pulse repetition intervals (PRIs), Radon-Fourier transform (RFT), blind speed side lobe (BSSL).

I. INTRODUCTION

In radar signal processing, long-time signal integration can effectively improve the signal-to-noise ratio (SNR) of the system and improve the detection ability of low observable targets. There are two common integration algorithms: coherent integration and incoherent integration. The performance of coherent integration is better than incoherent integration, it is an optimal energy integration method and has been extensively and deeply studied [1], [2].

Moving target detection (MTD) is the most commonly used coherent integration algorithm, which is simple and efficient. But the MTD algorithm is no longer applicable when the range migration effect occurs in a coherent integration period. In order to solve this problem, Keystone transform (KT) is used to compensate for the range migration, and then coherent integration is realized through MTD [3], [4]. However, due to the influence of Doppler ambiguity, this method is difficult to solve the range migration problem of multiple speed ambiguity targets [5]. Obviously, we can shorten the pulse repetition interval (PRI) to solve the Doppler ambiguity, but within the limitation of the hardware system, it is impossible to shorten the PRI indefinitely to avoid the Doppler ambiguity caused by the target with higher speed. The new coherent integration method based on Radon-Fourier transform (RFT) algorithm is proposed in [6]–[8], which extracts the target observations in the range-slow time plane according to the motion parameters of the targets. Then the observed values are integrated by the discrete Fourier transform (DFT) to achieve the long-time coherent integration of the target energy. The RFT method can significantly improve the detection ability for weak targets, and solve Doppler ambiguity at the signal level. Because of the superior performance of RFT, it has been studied and extended in many aspects. For example, the improved Radon-fractional Fourier transform method is proposed to detect the high-order moving targets [9], the fast implementation of generalized RFT method is designed to simplify the computational

The associate editor coordinating the review of this manuscript and approving it for publication was Weimin Huang.

complexity of the algorithm [10], and the space-time RFT method is used to achieve multi-dimensional coherent integration of targets [11], etc. In general, all these RFT applications achieve long-time coherent integration and focus before the detection of targets [12], [13].

However, in practical applications, affected by discrete pulse sampling, limited integration pulse number and finite range resolution, the output of RFT is always accompanied by blind speed side lobe (BSSL), which affects the final detection performance. In order to suppress the BSSL, the paper [7] proposed a windowing method, but it still remains large side lobe and causes the SNR loss for target detection. As we know, multiple PRIs are often used to solve velocity ambiguities. Reference [14] uses the same transmitter to transmit multiple PRI signals to increase the maximum unambiguous velocity, thus avoiding the problem of velocity ambiguity. Reference [15] adopts two different PRI signals as transmit signal, according to the equation relationship between the maximum unambiguous velocity and the ambiguous velocity of the different PRIs, the real velocity is obtained, which is most commonly used in radar signal processing to solve velocity ambiguities. However, multiple PRIs also can be used in RFT processing to suppress BSSL. For example, reference [16] proposed a method based on random repetition intervals, this method solves the velocity ambiguity and BSSL suppression problems via adding random jitter on uniform PRI. The system PRI of this method is constantly changing, which leads to the subsequent signal processing algorithm being more complicated, it is difficult to implement in practical engineering applications. The RFT method combined with two different PRIs (2RFT) is proposed in [17], [18], this method can completely suppress the BSSL and is simple to implement, but it cannot detect the target with speed on one of the PRI's Doppler blind speed bands.

Aiming at the above problems, this paper proposes an improved multiple pulse repetition intervals RFT (MRFT) method. This method uses multi-PRIs Linear frequency modulated (LFM) signals as transmitted radar signal and jointly processes the RFT outputs in different PRIs. By compensating the target's range migration in different PRIs, the locations of BSSL should not overlap due to the properly designed PRI. Then the BSSL suppression and SNR improvement are achieved easily via some minimizing and maximizing operations on the multi-PRIs RFT outputs. Because the target has been compensated to the same location in different PRIs, the minimizing and maximizing operations should have little effect on target's main lobe, therefore this method can preserve the coherent integration gain improved by RFT processing. Furthermore, the experimental results demonstrate the effectiveness of the MRFT method designed in this paper.

The remainder of this paper is organized as follows. In Section II, the signal model is given and deduced in detail. In Section III, the definition of RFT is introduced, the causes of BSSL and the characteristics of BSSL are also discussed. Section IV presents the limitations of 2RFT method for BSSL suppression, and the MRFT coherent integration method is proposed. Meanwhile, the design rules of the three PRIs are also analyzed. In Section V, comparison results are provided by using simulation and real measured numerical experiments to validate our MRFT coherent integration method. Finally, some conclusions are drawn in Section VI.

II. SIGNAL MODEL

For the signal model of the LFM system which is commonly used in many fields [19]–[21], the radar transmitted signal is

$$s_t(t) = \mathrm{rect}\left(\frac{t}{T_p}\right)\exp\left\{j2\pi\left[f_c t + \frac{1}{2}k_r t^2\right]\right\} \tag{1}$$

where rect $(\cdot)$ is rectangle function, T_p is the pulse width of the modulation signal, $k_r = B/T_P$ is the frequency modulated rate, B is the bandwidth of the transmitted signal. Therefore, the received echoes of the point target with uniform rectilinear motion can be described as

$$s_r(t,\tau) = \sigma_r \mathrm{rect}\left(\frac{T-\tau}{T_P}\right)\exp\left\{j2\pi\left[f_c(t-\tau)+\frac{k_r}{2}(t-\tau)^2\right]\right\} \tag{2}$$

where σ_r is the amplitude of the target, $\tau = 2r(t_m)/c$ is the time delay, and $r(t_m) = r_0 + v_0 t_m$ is the real-time range of the target, r_0 and v_0 are the initial range and radial speed, $t_m = mT_r$ is the slow time, m $= 0, 1, 2, \ldots N_m - 1$ is the number of coherent integration pulses, T_r is the pulse repetition time, and $t = \mathrm{n}t_s$ is the fast time, n $= 0, 1, 2, \ldots N_n - 1$ is the number of fast time sampling points, t_s is the fast time sampling interval.

After demodulation and pulse compression, then insert $\tau = 2r(t_m)/c$ into the equation (2) to get the time-domain signal with m integrated pulses

$$s_{pc}(t, t_m) = A_r \mathrm{sinc}\left[B\left(t - \frac{2r(t_m)}{c}\right)\right]\cdot\exp\left(-j4\pi f_c \frac{r(t_m)}{c}\right) \tag{3}$$

where $A_r$sinc $(\cdot)$ contains the amplitude envelope information of targets, the index term represents the range and Doppler information of targets.

In the LFM system, $\Delta \mathrm{r} = c/2B$ is the range resolution, when the offset exceeds the range resolution, the range migration effect will occur, which creates difficulties during the long-time coherent integration processing. In this context, the RFT algorithm is proposed.

III. RFT AND BSSL

A. THE DEFINITION OF RFT

The basic principle of RFT is that it compensates the phase of the signal in the coherent integration period according to the moving speed of the target [10], then integrates the motion trajectory of the target along with the range and slow time dimension to obtain a focused target point. The definition of standard RFT for the uniformly moving target is as follow

$$\mathrm{G}(r, v) = \int s_{pc}\left[\frac{2(vt_m + r)}{c}, t_m\right]\exp(-j2\pi f_d t_m)\, dt_m \tag{4}$$

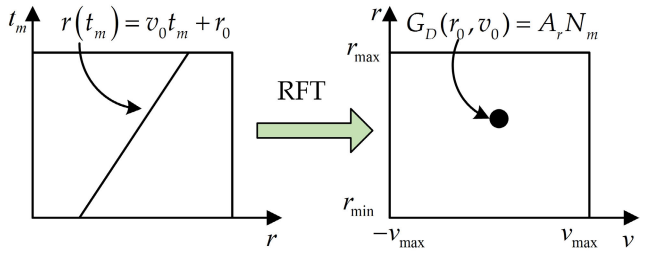

FIGURE 1. The RFT working diagrammatic sketch.

where s_{pc} is the pulse compression result same to the equation (3), f_d is the Doppler frequency, v represents the searching speed, the region is $[-v_{\max}, v_{\max}]$, and r is the searching range, the region is $[r_{\min}, r_{\max}]$. Therefore, the RFT processing can extract the observation values in the range-slow time plane and integrate the energy of target as a peak. Finally, we can get the output $G_D(r_0, v_0) = A_r N_m$, which is the energy integration of N_m pulses at the true range and speed location of the target [8], the energy of the target signal is enhanced. The RFT working diagrammatic sketch can be represented in Fig.1, it shows that the $r - t$ parameter space is converted to the $r - v$ parameter space by RFT processing. In the $r - v$ parameter space, a sharp peak is generated through the long-time coherent integration for the target trajectory with uniform linear motion [22].

B. THE GENERATION OF BSSL

From the above description, it can be seen that the RFT output obtains the coherent integration gain at the target location. At the same time, some integration gain is also generated at the ambiguity speed, i.e., $v(k) = v_0 + kv_b$, which is called BSSL, where $v_b = \lambda/2T_r$ is the blind speed, $k = 0, \pm1, \pm2, \cdots \pm k_{max}$ is the blind speed ambiguity integer. Then insert $v(k)$ into equation (4), we can obtain that

$$\begin{aligned} &\mathrm{G}(r, v(k)) \\ &= \int s_{pc}\left[\frac{2(r + v(k)\, t_m)}{c}, t_m\right] \cdot exp\left(-j\frac{4\pi v(k)\, t_m}{\lambda}\right) dt_m \\ &= A_r \int \mathrm{sinc}\left\{2\pi B\left[\frac{r - r_t - kv_b t_m}{c}\right]\right\} dt_m \\ &\approx A_r \sum_{m=0}^{N_m - 1} \mathrm{rect}\left(\frac{r - r_t - kv_b t_m}{\Delta r}\right) \end{aligned} \tag{5}$$

Form equation (5) it is clear that the RFT processing can get the ideal integration result when $k = 0$ and $r = r_0$. However, if $k \neq 0$, the peak location of the rect $(\cdot)$ function would vary with t_m. At this point, there will be some BSSL peaks, which will generate false alarms when it is larger than the decision threshold of the detector.

C. THE CHARACTERISTICS OF BSSL

In order to understand the distribution characteristics of BSSL in more detail, the range resolution, speed resolution and amplitude of BSSL need be analyzed, which can provide the theoretical basis for the BSSL suppression [23].

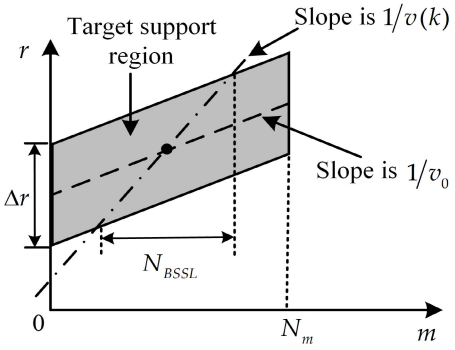

FIGURE 2. The sketch map of the integration path in RFT.

For a coherent integration period of RFT, the parameter of rect $(\cdot)$ function, i.e., $m_1 = 0$, $m_2 = N_m$, represent the beginning and ending pulse of the coherent integration, respectively. Then we can get the corresponding range as $r_1 = r_t - \Delta r/2$, $r_2 = r_t + |k|\, v_b N_m T_r + \Delta r/2$, and the range resolution of BSSL is obtained

$$\Delta r_{BSSL} = r_2 - r_1 = |k|\, v_b N_m T_r + \Delta r \quad k \neq 0 \tag{6}$$

From (6), we can know that the range resolution of BSSL increases with $|k|$.

As for the amplitude and speed resolution of BSSL, we first need to know the integrated pulse number of BSSL, it can be obtained by analyzing the integration paths of BSSL. Therefore, based on the working principle of RFT, the RFT integration paths can be represented in Fig. 2, where the shadow part is the target support region, and the slope of two integration paths are $1/v_0$ and $1/v(k)$, respectively.

From Fig. 2, it is clear that the ideal integration path of the target support region is the line that slope is $1/v_0$,. As for the BSSL integration path, the slope is $1/v(k)$, $k \neq 0$, which has N_{BSSL} intersection points with the target support region. By performing a simple geometry analysis of Fig. 2, we can get the equation as

$$N_{BSSL} T_r v_0 + \Delta r = N_{BSSL} T_r v(k) \tag{7}$$

Then insert $v(k) = v_0 + kv_b$ into equation (7), the integration number of BSSL can be calculated as

$$N_{BSSL} = \frac{\Delta r}{|v(k) - v_0|\, T_r} = \frac{\Delta r}{|k|\, v_b T_r} = \frac{2\Delta r}{|k|\, \lambda} \quad k \neq 0 \tag{8}$$

Therefore, the amplitude of BSSL can be expressed as

$$|G_{BSSL}(r, v(k))| = A_r \cdot N_{BSSL} = \frac{2A_r \Delta r}{|k|\, \lambda} \quad k \neq 0 \tag{9}$$

The speed resolution of BSSL can be derived from the speed resolution of RFT. It is known that the speed resolution of RFT is similar to the MTD method, which can be expressed as follow

$$\Delta v_{RFT} = \frac{\lambda}{2NT_r} \tag{10}$$

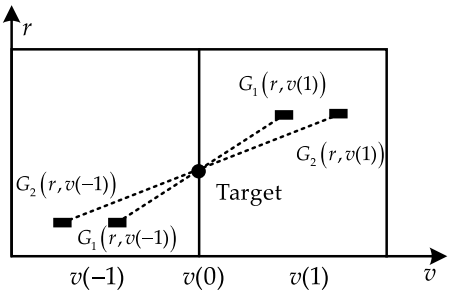

FIGURE 3. The BSSL distribution diagram of two different PRIs.

where N is the number of integrated pulses. Then replace N with N_{BSSL}, the speed resolution of BSSL can be obtained as

$$\Delta v_{BSSL}(k, T_r) = \frac{\lambda}{2N_{BSSL}T_r} = \frac{\lambda^2 |k|}{4\Delta r T_r} \tag{11}$$

It is obvious that the speed resolution of BSSL increases with the speed blind ambiguity integer $|k|$, and decreases with the pulse repetition interval T_r.

IV. PROPOSED METHOD

In this section, the limitations of the 2RFT method for BSSL suppression are discussed, then based on the distribution characteristics of BSSL, our improved MRFT method with three different PRIs is proposed. In addition, the design criteria of three PRIs are also analyzed.

A. LIMITATIONS OF THE 2RFT METHOD FOR BSSL SUPPRESSION

From the previous analysis of BSSL, we can see that the locations of BSSL are related to blind speed, where the blind speed is determined by the PRI. For different PRIs, the target's main lobes are compensated by RFT to the r-v positions of same absolute time, which can be the beginning time or ending time of the coherent integration, thus the main lobe locations of different PRIs are same in the same integration period. However, since the corresponding BSSLs are not real targets, they cannot be compensated to the same locations by RFT. Therefore, we can suppress BSSL by minimizing operation on the RFT outputs of different PRIs. However, the number of PRIs is an issue that needs to be further discussed.

Suppose there are two alternately transmitted PRIs, i.e., T_1 and T_2, where $T_1 > T_2$, $G_1(r, v)$, $G_2(r, v)$ are the RFT outputs of two different PRIs, respectively, the distribution diagram is given in Fig. 3. It can be seen that the target's main lobe of the two PRIs is focused in the $v(0)$ line, while the BSSL locations are different in $v(-1)$ and $v(1)$ regions.

Based on the location differences of BSSL with different PRIs, a minimizing operator is constructed on the two different RFT outputs, i.e., $G_1(r, v)$ and $G_2(r, v)$, then we get the minimizing result as below

$$G_{12}(r, v) = \min\left(|G_1(r, v)|, |G_2(r, v)|\right) \tag{12}$$

As for the minimizing operation, what needs to be explained is that the range migration between different PRIs has been compensated by the RFT processing. Therefore, the locations and the amplitude of the target's main lobe in the two PRIs are assumed to be the same. Consequently, the amplitude of the main lobe will not be reduced by minimizing operation.

For the case that the speed of the target's speed is not on the two PRIs' blind speed band, i.e., $v_0 \neq kv_b, k = \pm 1, \pm 2, \cdots \pm k_{\max}$, the minimizing result will hold the main lobe of the target, while the BSSL is suppressed, then the target can be easily detected. However when the target's speed is on one of the two PRI's blind speed band, i.e., $v_0 = kv_b$, $k = \pm 1, \pm 2, \cdots \pm k_{\max}$, the targets and BSSLs would be filtered out as stationary targets by the corresponding Doppler filter. Therefore, the minimizing result of two PRI's RFT outputs cannot preserve the target. In summary, the 2RFT method can remove the BSSL of the targets with speed not on their blind speed band by minimizing operation, but it is not useful for the targets with speed on its blind speed band.

B. PROPOSED IMPROVED MRFT COHERENT INTEGRATION METHOD

Aiming at the limitations of the 2RFT method, we proposed an improved MRFT method with three alternately transmitted PRIs, i.e., T_1, T_2 and T_3, where $T_1 > T_2 > T_3$. The RFT outputs of three different PRIs are $G_1(r, v)$, $G_2(r, v)$ and $G_3(r, v)$. Firstly, construct three minimizing operators of each two on the three RFT outputs, it will generate three results

$$\begin{aligned} G_{12}(r, v) &= \min\left(|G_1(r, v)|, |G_2(r, v)|\right) \\ G_{13}(r, v) &= \min\left(|G_1(r, v)|, |G_3(r, v)|\right) \\ G_{23}(r, v) &= \min\left(|G_2(r, v)|, |G_3(r, v)|\right) \end{aligned} \tag{13}$$

For the case that $v_0 \neq kv_{bn}, k = \pm 1, \pm 2, \cdots \pm k_{max}$, $n = 1, 2, 3$, all the three minimizing results have the target's main lobe, and the BSSLs are suppressed. If $v_0 = kv_{bn}$, suppose $n = 1$, it means that the target's speed is on the blind speed band of the first PRI, it is clear that the RFT output of first PRI does not keep the target and BSSL, and therefore the target's main lobe in the minimizing results $G_{12}(r, v)$ and $G_{13}(r, v)$ will be removed. Fortunately, since we have three sets of minimizing results, there is still a set of result, i.e., $G_{23}(r, v)$ hold the target's main lobe. Consequently, we can construct a maximizing operator on the three sets of minimizing results to extract out the target, as shown in the following equation (14).

$$G_{123}(r, v) = \max\left(G_{13}(r, v), G_{13}(r, v), G_{23}(r, v)\right) \tag{14}$$

Therefore, the main lobe of the target can be preserved, and the target's true range and speed can get through Constant False Alarm Rate (CFAR) processing. Similarly, when the target's speed is on the blind speed of second PRI or third PRI, the same results can be obtained.

However, the premise of constructing minimizing operators on three RFT outputs is that the BSSL locations of

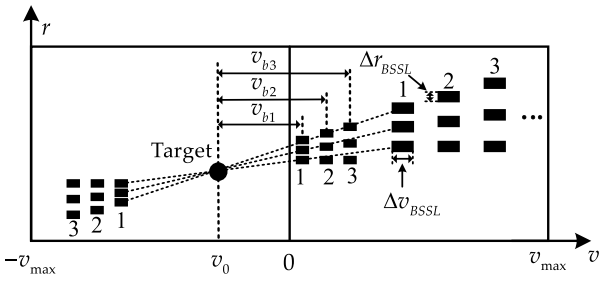

FIGURE 4. Three different PRI's BSSL distribution diagram.

different PRIs are distinguishable. Therefore, the three different PRIs must be designed reasonably to avoid BSSL overlap, and its detailed analysis is as follows. Meanwhile, the selection of optimal PRIs is also analyzed.

Suppose v_{b1}, v_{b2} and v_{b3} are the blind speed of three different PRIs, respectively, where $v_{b1} < v_{b2} < v_{b3}$. The BSSL distribution diagram of three different PRIs can be described as Fig. 4, where the speed searching region is $-v_{max}$ to v_{max}, the figures in Fig. 4 are used to label the BSSL of three different PRIs. Moreover, the speed difference between the main lobe of the target and BSSL band is $|k|\, v_b$, where $v_b \in (v_{b1}, v_{b2}, v_{b3})$, $k \neq 0$. For the BSSL points, the width of BSSL represents its speed resolution, and the height of BSSL represents its range resolution, both of which are linearly proportional to the blind speed ambiguity integer $|k|$. In addition, the number of BSSL points on a BSSL band depends on the number of coherent processing intervals (CPIs) integrated by the RFT. In practical applications, it is common to combine multiple CPIs to improve the coherent integration time, Fig. 4 shows the result of integrating three adjacent CPIs.

From Fig. 4, we can know that the BSSL band of $k > 0$ and $k < 0$ are symmetric about the target's main lobe, thus we only discuss the BSSL with $k > 0$. Suppose the third PRI T_3 is known, the other two PRI T_1 and T_2 are unknown. According to the positional relationship of BSSL in Fig. 4, the condition that the BSSL corresponding to three different PRIs does not overlap in the speed resolution unit can be expressed as

$$\begin{cases} (k+1)\, v_{b1} - k v_{b3} > \dfrac{\Delta v_{BSSL}(k, T_3) + \Delta v_{BSSL}(k+1, T_1)}{2} \\ k v_{b2} - k v_{b1} > \dfrac{\Delta v_{BSSL}(k, T_1) + \Delta v_{BSSL}(k, T_2)}{2} \\ k v_{b3} - k v_{b2} > \dfrac{\Delta v_{BSSL}(k, T_2) + \Delta v_{BSSL}(k, T_3)}{2} \end{cases} \tag{15}$$

Substitute equation (11) into equation (15) yields

$$\begin{cases} \dfrac{4\Delta r + \lambda}{4\Delta r - \lambda} T_3 < T_2 < \dfrac{4\Delta r - \lambda}{4\Delta r + \lambda} T_1 \\ T_1 < T_3 \dfrac{(4\Delta r - \lambda)(k+1)}{(4\Delta r - \lambda) k} \end{cases} \tag{16}$$

where $-k_{\max} \leq k \leq k_{\max}$, the $k_{\max}$ can be obtained by the maximizing measurement speed $v_{\max}$ and the maximizing blind speed v_{b3}, as shown in the following equation (17),

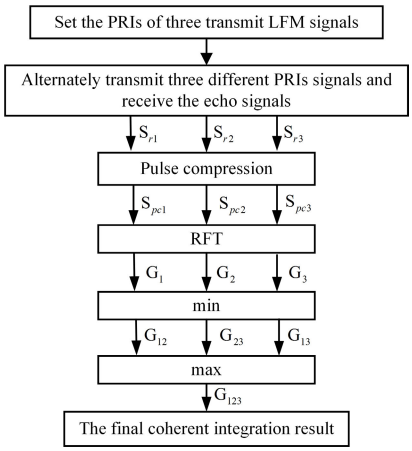

FIGURE 5. The overall flow of the proposed MRFT method.

where the ceil $(\cdot)$ is an up-round function. In addition, $k_{\max}$ can replace the k in equation (16) to further constrain the range of T_1 and T_2.

$$k_{\max} = \text{ceil}\left(\frac{v_{\max}}{v_{b3}}\right) \tag{17}$$

About the problem of selecting optimal PRIs, it can be transformed into constructing the optimal minimizing operator problem. For our system, under the constraints of three PRIs, if v_{b1} and v_{b2}, or v_{b2} and v_{b3} are very close, the external side lobes of BSSL resolution units between them will overlap partially, affecting the minimizing results. When $v_{b2} = (v_{b1} + v_{b3})/2$, the three BSSLs distribute equally in the speed dimension, and therefore the overlap area of the external side lobes are minimum, the best BSSL suppression effect can be achieved by minimizing operation. Therefore, under the constraints of the three PRIs, the optimal relationship of the three PRIs is $T_2 = (T_1 + T_3)/2$.

Based on the discussions and analysis above, we could design the appropriate T_1 and T_2 value to ensure that BSSLs are distributed in different speed resolution units in the three RFT outputs.

In summary, the overall flow of the improved MRFT coherent integration can be expressed as Fig. 5.

Furthermore, the truth table of this MRFT method can be obtained as follow Table 1. In Table 1, v_{b1}, v_{b2}, v_{b3}, and others denote the speed of targets, $G_{12}(r, v)$, $G_{13}(r, v)$ and $G_{23}(r, v)$ denote the different intermediate results in the proposed method, $G_{123}(r, v)$ is the final processing output, as discussed above, where 1 denotes the target is retained, 0 denotes the target is filtered out. It can be seen clearly from Table 1, the final processing output of our method can retain the target and suppress the BSSL, regardless of whether the speed is on the blind speed band or not, which overcomes the defect of the 2RFT method with two PRIs that cannot detect the targets with speed on their blind speed band.

V. NUMERICAL EXPERIMENTS

This section is devoted to evaluating the performance of the proposed MRFT coherent integration method via detailed

TABLE 1. The truth table of the proposed MRFT method.

	$G_{12}(r,v)$	$G_{13}(r,v)$	$G_{23}(r,v)$	$G_{123}(r,v)$
v_{b1}	0	0	1	1
v_{b2}	0	1	0	1
v_{b3}	1	0	0	1
others	1	1	1	1

numerical experiments, where the main system parameters of an experimental midrange searching radar are given as follows: the radar system works at X band with 10MHz instantaneous bandwidth, the range resolution is 15m. There are 90 integrated pulses in each CPI, and the waveform sequence is 90 pulses with first PRI, then 90 pulses with second PRI and 90 pulses with third PRI. The signal generator is the commonly used phase-locked loop (PLL), and we use three control instructions to control the PLL to generate three LFM signals with different PRI alternately. This technology is not complicated, and it has a mature application. Since the LFM signals are transmitted alternately, it also receives and processes echo signals alternately. Therefore, only one sampler can sample the three different PRI signals, the successive processing also reduces the demand for the processor, which has a low hardware complexity requirement. We set our experimental object is an unmanned aerial vehicle (UAV), its speed is usually between 10 and 20m/s. In order to verify our MRFT method can detect the target that speed on their blind speed band, we set the blind speed of three different PRIs between 10 and 20m/s. According to the system parameters, the constraints and the optimal relationship of the three PRIs, the blind speed v_{b1}, v_{b2}, v_{b3} can be set as 12.5m/s, 14.5m/s, 16.5m/s, and the three different PRI T_1, T_2, T_3 are 1.127ms, 1ms, 0.873ms, respectively. However, the values of the three PRI are not fixed, they can also be other values according to the real measurement situation. In addition, we set the maximum unambiguous measurement speed is $v_{\max} = 30m/s$, then insert the maximum blind speed v_{b3} and $v_{\max}$ into equation (17), we can get the maximum k is $k_{\max} = 2$.

The verification experiments of the proposed MRFT coherent integration method consists of two parts, the simulation experiment and the real measured experiment, and their system parameters are the same. In addition, the key object of our experiments are the targets with speed on their blind speed band. At the same time, we will also use the 2RFT method to process the data, where the two PRIs are T_1 and T_2, respectively, then compare the coherent integration performance of the two methods.

A. SIMULATION EXPERIMENT

The simulation experiment includes two parts: one is to verify the BSSL suppression performance and the other is to verify the SNR improvement performance of the MRFT coherent integration method.

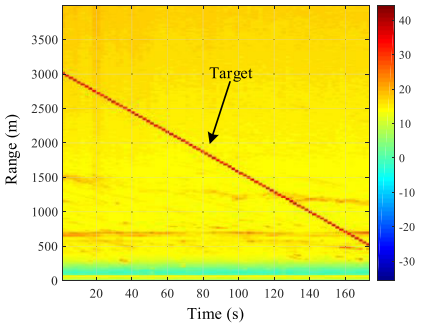

FIGURE 6. The target trajectory of simulation data.

Firstly, the simulation experiments are well-designed to evaluate the BSSL suppression performance of the MRFT method, where the experimental data are derived from the real measured background data with simulation targets in uniform linear motion, and the simulation parameters are same to the real radar system parameters. Set the initial distance of the simulation target is 3000m, the initial radial speed is -14.5m/s, where the speed is on the blind speed band of the second PRIs. About the sign of speed, we define the speed is negative when the targets are close to the radar system, otherwise the opposite. In addition, it is assumed that the target has the same speed and radar cross section (RCS) in the same CPI, and move in the same radar beam range.

For the data obtained from simulation, Moving Target Indicator (MTI) processing is carried out to filter out the static clutter, which is widely used in modern radar signal processing as a mature Doppler filtering technology to cancel clutter. The target trajectory after MTI processing is shown in Fig. 6, it represents the energy of the simulation signal, where the unit of the color bar in the right of the figure is dB. In addition, Fig. 6 vividly shows the time-range variation of the target moving near the radar system from 3000m to 500m.

Take RFT processing to the simulation data, where the range searching region is $[0m, 4000m]$, and the speed searching region is $[-30m/s, 30m/s]$. Then the RFT outputs and incoherent integration results of three different PRIs are obtained as Fig. 7, where the CPI number of coherent integration is 5, therefore a BSSL band consists of five BSSL points. Since the target's speed is on the blind speed band of the second PRI, the target and BSSL are filtered out by the MTI in the RFT output $G_2(r, v)$, as depicted in Fig. 7 (b). However, the target and BSSL are kept in the RFT output $G_1(r, v)$ and $G_3(r, v)$, as illustrated in Fig. 7 (a) and (c), cause the target's speed are not on their blind speed band. In addition, for the convenience of observation and comparison, the three RFT outputs are integrated incoherently, the top view of the result is given in Fig. 7 (d). It can be seen from Fig. 7 (d) that the target main lobe of different PRIs is in the same location, while the BSSLs are in different locations, which is consistent with the theoretical analysis in section IV.

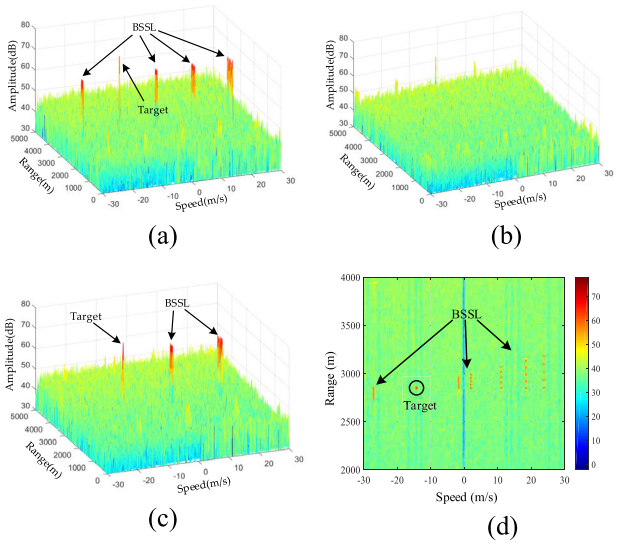

FIGURE 7. The RFT outputs of different PRIs. (a) The RFT output of first PRI $G_1(r, v)$. (b) The RFT output of second PRI $G_2(r, v)$. (c) The RFT output of third PRI $G_3(r, v)$. (d) The incoherent integration result of three RFT outputs.

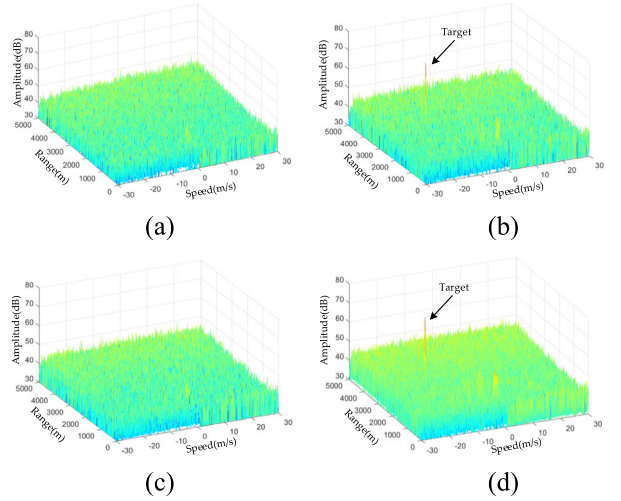

FIGURE 8. The processing results of different PRIs RFT outputs. (a) The minimizing result $G_{12}(r, v)$. (b) The minimizing result $G_{13}(r, v)$. (c) The minimizing result $G_{23}(r, v)$. (d) The maximizing result $G_{123}(r, v)$.

The next step is to construct minimizing and maximizing operators on the three RFT outputs according to the designed algorithm, then the processing results are given below.

Fig. 8 (a) is the minimizing result of $G_1(r, v)$ and $G_2(r, v)$, which is the final processing result of the 2RFT method, it is obvious that there is no target in the result. According to the above description, we can know that the target's main lobe and BSSL in the second's RFT result $G_2(r, v)$ be filtered out. Therefore, the minimizing result $G_{12}(r, v)$ will lose the target's main lobe. Consequently, the 2RFT method cannot detect the targets with speed on their blind speed band. Fig. 8 (c) gives the minimizing result of $G_2(r, v)$ and $G_3(r, v)$, which is same as Fig. 8 (a). However, benefit from the three different minimizing results in our proposed

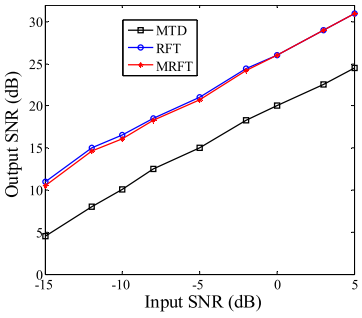

FIGURE 9. The output SNR of different coherent integration methods.

MRFT method, the target is preserved in $G_{13}(r, v)$, as shown in Fig. 8 (b). Fig. 8 (d) is the final result $G_{123}(r, v)$ what we get via a maximizing operation on the three minimizing results, it shows that the BSSLs are successfully suppressed and the target's main lobe is retained.

Moreover, to evaluate the SNR improvement performance of our MRFT method, we design the experiments with different input SNR, then compare the output SNR of different coherent integration methods, where the number integrated CPIs is five, contains 450 pulses. The SNR of simulated input data after pulse compression is set as -15dB to 5dB, the output SNR of MTD, RFT and MRFT methods are illustrated in Fig. 9.

According to the theory of radar signal processing, the output SNR after coherent integration can be given as

$$SNR_{out} = SNR_{in} + 10 * log10\,(N_{all}) \tag{18}$$

where SNR_{in} is the SNR after pulse compression, N_{all} is the periodic number of coherent integration. For MTD, the integrated results diffuse in the range dimension due to the range migration of the target, only 90 pulses of each CPI achieve coherent integration, therefore the N_{all} is 90. For RFT and MRFT, the range migration is compensated, therefore the integrated CPI number is 5 and the N_{all} is 450. Consequently, it can be calculated that their theoretical coherent integration gains are 19.54dB and 26.53dB, respectively.

By comparing the SNR curve in Fig. 9, we could know that the experimental results agree perfectly with the theoretical analysis, the SNR improvement performance of RFT method is better than the MTD method. Furthermore, the output SNR curves of RFT and MRFT are very close, which indicates that the proposed MRFT method does not lose the signal gains improved by RFT.

B. REAL MEASURED EXPERIMENT

The experimental scene of the real measured data is an open wetland environment, and the target is a multi-rotor UAV, the details are shown in Fig. 10 below. The wetland environment has many trees, they will cause a lot of clutters and reduces the system's signal-to-clutter ratio. In addition, the real measured target is a DJI Phantom UAV, it has small RCS and strong maneuverability. Our radar system has high pulse repetition frequency, and therefore the complex motion of UAV can be

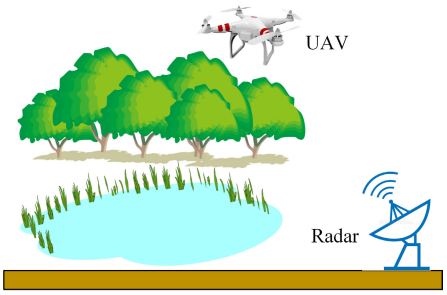

FIGURE 10. The real measured scene.

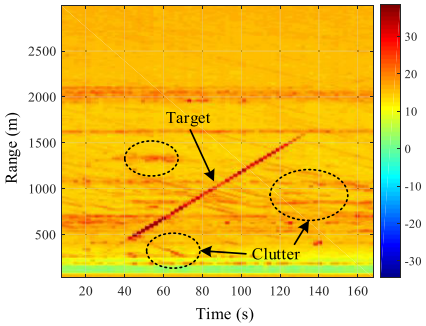

FIGURE 11. The target trajectory of real measurement data.

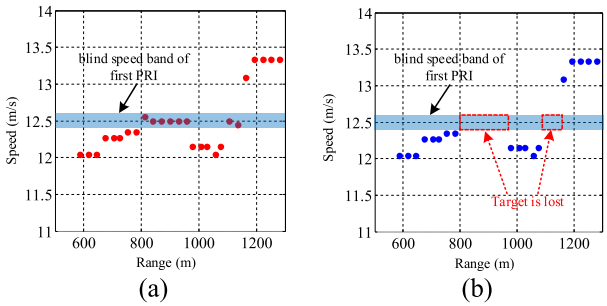

FIGURE 12. The range and speed distribution of the real measured target. (a) The processing results of the proposed MRFT method. (b) The processing results of the 2RFT method.

divided into many short-time uniform linear motion, it will be more suitable for MRFT processing.

We set the UAV to fly from 500m to 1500m with the speed about 12.5m/s, sample the real measured echoes and take MTI processing, then get the following target trajectory as Fig. 11. It can be seen that the real measured data contains a lot of moving clutters in the near range, and the target echo intensity change with the environment. Those interferences will make signal processing more difficult.

The 2RFT and MRFT processing are carried out to the real measured data, where the range searching region is $[0m, 3000m]$, and the speed searching region is $[-30m/s, 30m/s]$. To compare the BSSL suppression and SNR improvement performance of the two methods, we take a more detailed analysis for the processing results. Firstly, the detection results of the two methods are illustrated in Fig 12. Ideally, the UAV should fly with the speed is 12.5m/s.

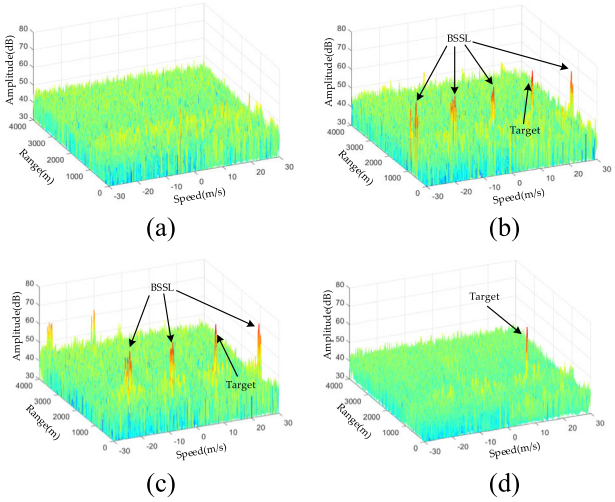

FIGURE 13. The RFT outputs of different PRIs. (a) The RFT output of first PRI $G_1(r, v)$. (b) The RFT output of second PRI $G_2(r, v)$. (c) The RFT output of third PRI $G_3(r, v)$. (d) The final processing result of the proposed method.

However, Fig 12 shows that the speed of the target varies in a small speed region around 12.5m/s, mainly because the target is disturbed by the wind and other external factors, therefore it cannot fly uniformly as we set.

By comparing the Fig 12 (a) and (b), it is clear that when the target's speed is on the blind speed band of first PRI, the 2RFT method with two PRIs causes the target to be lost, which results in a large missing alarm rate, while the MRFT proposed in this paper does not lose any targets. Based on this situation, a detailed analysis of the target point that on the blind speed band is performed, and the processing results are given in Fig 13.

Fig 13. gives the three RFT outputs and the final processing result, where Fig 13. (a) is the RFT outputs of the first PRI, which filter out the target that speed is on their blind speed band. However, because the second and third blind speeds are different from the target speed, the target's main lobe and BSSL are preserved in Fig 13. (a) and (b). By carefully observing the BSSL points in Fig 13. (a) and (b), it can be found that, unlike the simulation data, the amplitude of BSSL points in a BSSL band are not same, it is mainly due to the change of RCS caused by target jitter in the integrated CPIs, which is quite normal in practical application and it would not affect the coherent integration. At last, Fig 13. (d) represents the final processing output of proposed MRFT method, it shows that the real measured target that speed is on the first PRI's blind speed band is successfully retained and BSSL suppression is achieved.

In order to analyze the BSSL suppression performance of the proposed MRFT method more intuitively, we compare the amplitude change of the BSSL points before and after the MRFT processing, then get Table 2 as below. In Table 2, the $|G_2(-2)|$, $|G_2(-1)|$, and so on are the mean of the BSSL band's amplitude in $G_2(r, v)$ and $G_3(r, v)$, respectively, the amplitude of the target main lobe is also listed.

TABLE 2. The comparison of amplitude before and after MRFT processing (dB).

	$\|G_2(-2)\|$	$\|G_2(-1)\|$	$\|G_2(1)\|$	$\|G_3(-2)\|$	$\|G_3(-1)\|$	$\|G_3(1)\|$	Target	Average noise
before	66.18	66.57	66.87	66.33	65.76	66.34	74.38	38.38
after	44.87	37.70	42.15	44.09	40.12	41.11	73.9	38.69
difference value	21.31	28.87	24.72	22.24	25.64	25.23	0.48	-0.31

TABLE 3. The detection performance of different methods.

Method	detection rate	false alarm rate	missed detection rate
2RFT	69.23%	0.0381%	30.77%
MRFT	100%	0.0305%	0

From the BSSL suppression values, we can see that the BSSL has been suppressed a lot, the amplitude of BSSL points after suppression is close to the average noise value. Moreover, the amplitude of target main lobe and average noise has not changed too much, which means that our processing does not lose the SNR improved by long-time coherent integration. In summary, the comparison results further validate the performance of our MRFT coherent integration method.

Furthermore, both the 2RFT method detection results and MRFT method detection results of the real measured target moved around the blind speed band are summarized in Table 3, which includes three indicators: the detection rate P_d, the false alarm rate P_f and the missed detection rate P_m, their formulas are as equation (18).

$$\begin{cases} P_d = N_{dT} / N_T \\ P_f = \frac{1}{N} \sum_{n=0}^{N-1} \left(N_{fTn} / N_{alln} \right) \\ P_m = 1 - P_d = N_{mT} / N_T \end{cases} \tag{19}$$

where N_{dT}, N_{mT} and N_T denote respectively the number of detected real targets, the number of missed real targets, the total number of real targets in all frames. In addition, N is the total number of the processing frames, N_{fTn} is the falsely detected targets number of the nth frame, and N_{alln} is the non-targets points number in the r-v plane of the nth frame, where the r-v plane is the RFT processing output. However, in our experiments, there are fewer target points in each frame. For the convenience of calculation, N_{alln} can usually be set as the total points number in the r-v plane, which includes a very small number of target points and most non-target points.

The detection results show that RFT processing can ensure the target detection has a lower false alarm rate. Obviously, the detection result of the 2RFT method has higher missed detection rate, but our MRFT method has a higher detection rate. It is shown that the MRFT method is useful for detecting the targets with speed on the blind speed band.

The above numerical experiment results show that the MRFT method designed in this paper has good performance for the targets with speed on their blind speed band, whether in the scenario with ideal simulation targets or in the real complex scenarios with irregular moving UAV targets, which verify the effectiveness of our algorithm. It is no doubt that the method is also suitable for the targets whose speed is not on the blind speed band.

VI. CONCLUSION

As a long-time coherent integration method, RFT has a good effect on the detection of weak and highly maneuverability targets in a complicated environment. However, the RFT method still has serious BSSL problems need to be solved. The theoretical analysis shows that the different blind speed determines the BSSL of RFT outputs appears in different locations. In view of this, the MRFT method with three different PRIs is proposed. First set the appropriate PRIs, alternately transmit and receive radar signals, take RFT processing on the received signals, then construct the minimizing and maximizing operators on the three RFT outputs. Finally, BSSL suppression and SNR improvement are achieved easily. Compare with the processing results of the 2RFT method with two different PRIs in [17], [18], our MRFT method can solve the BSSL problems of the targets with speed on the blind speed band, and reduce the missed detection rate. Compare with the traditional MTD method, our MRFT method can significantly improve the SNR and reduce the false alarm rate of the system. In summary, through our theoretical analysis and numerical experiments, it can be known that the proposed MRFT method can suppress BSSL, improve system SNR and detection rate effectively, it can be wildly used in RFT processing to improve the targets detection performance. However, our current research is based on approximating the motion of the targets to a number of short-time uniform linear motion. In the future, further study is needed for more complex motion.

REFERENCES

[1] X. Chen, J. Guan, X. Li, and Y. He, "Effective coherent integration method for marine target with micromotion via phase differentiation and radon-Lv's distribution," *IET Radar, Sonar Navigat.*, vol. 9, no. 9, pp. 1284–1295, Oct. 2015.

[2] R. P. Perry, R. C. Dipietro, and R. L. Fante, "SAR imaging of moving targets," *IEEE Trans. Aerosp. Electron. Syst.*, vol. 35, no. 1, pp. 188–200, Jan. 1999.

[3] R. P. Perry, R. C. Dipietro, and R. L. Fante, "Coherent integration with range migration using keystone formatting," in *Proc. IEEE Radar Conf.*, Boston, MA, USA, Apr. 2007, pp. 863–868.

[4] W. Li, W. Zhang, and Z. Jiao, "High speed maneuvering target detection based on the modified keystone transform," in *Proc. IEEE ISCID*, Hangzhou, China, Dec. 2017, pp. 114–118.

[5] S. B. Peng, J. Xu, X.-G. Xia, F. Liu, T. Long, J. Yang, and Y.-N. Peng, "Multiaircraft formation identification for narrowband coherent radar in a long coherent integration time," *IEEE Trans. Aerosp. Electron. Syst.*, vol. 51, no. 3, pp. 2121–2137, Jul. 2015.
[6] J. Xu, J. Yu, Y.-N. Peng, and X.-G. Xia, "Radon-Fourier transform for radar target detection, I: Generalized Doppler filter bank," *IEEE Trans. Aerosp. Electron. Syst.*, vol. 47, no. 2, pp. 1186–1202, Apr. 2011.
[7] J. Xu, J. Yu, Y. N. Peng, and X. G. Xia, "Radon-Fourier transform for radar target detection (II): Blind speed sidelobe suppression," *IEEE Trans. Aerosp. Electron. Syst.*, vol. 47, no. 4, pp. 2473–2489, Oct. 2011.
[8] J. Yu, J. Xu, Y.-N. Peng, and X.-G. Xia, "Radon-Fourier transform for radar target detection (III): Optimality and fast implementations," *IEEE Trans. Aerosp. Electron. Syst.*, vol. 48, no. 2, pp. 991–1004, Apr. 2012.
[9] X. Chen, F. Cai, Y. Cong, and J. Guan, "Radon-fractional Fourier transform and its application to radar maneuvering target detection," in *Proc. IEEE Int. Conf. Radar*, Adelaide, SA, Australia, Sep. 2013, pp. 346–350.
[10] L.-C. Qian, J. Xu, X.-G. Xia, W.-F. Sun, T. Long, and Y.-N. Peng, "Fast implementation of generalized radon-Fourier transform for maneuvering radar target detection," *Electron. Lett.*, vol. 48, no. 22, pp. 1427–1428, Oct. 2012.
[11] J. Xu, J. Yu, Y.-N. Peng, X.-G. Xia, and T. Long, "Space-time radon-Fourier transform and applications in radar target detection," *IET Radar Sonar Navigat.*, vol. 6, no. 9, pp. 846–857, Dec. 2012.
[12] J. Xu, Y. N. Peng, X. G. Xia, and A. Farina, "Focus-before-detection radar signal processing: Part I—Challenges and methods," *IEEE Aerosp. Electron. Syst. Mag.*, vol. 32, no. 9, pp. 48–59, Sep. 2017.
[13] J. Xu, Y. Peng, X. Xia, T. Long, E. Mao, and A. Farina, "Focus-before-detection radar signal processing: Part II—Recent developments," *IEEE Aerosp. Electron. Syst. Mag.*, vol. 33, no. 1, pp. 34–49, Jan. 2018.
[14] I. Shapir, I. Bilik, and G. Barkan, "Doppler ambiguity resolving in TDMA automotive MIMO radar via digital multiple PRF," in *Proc. IEEE Radar Conf. (RadarConf)*, Oklahoma City, OK, USA, Apr. 2018, pp. 175–180.
[15] M. Kronauge and H. Rohling, "New chirp sequence radar waveform," *IEEE Trans. Aerosp. Electron. Syst.*, vol. 50, no. 4, pp. 2870–2877, Oct. 2014.
[16] Q. Kang, J. Xu, L. C. Qian, and M.-M. Bian, "Random carrier-frequency Radon-Fourier transform for radar target detection," in *Proc. IET Int. Radar Conf.*, Hangzhou, China, Oct. 2015, pp. 14–16.
[17] L. Qian, J. Xu, W. Sun, and Y. Peng, "Blind speed side lobe suppression in radon-Fourier transform based on radar pulse recurrence interval design," *J. Electron. Inf. Technol.*, vol. 34, no. 11, pp. 2608–2614, Nov. 2018.
[18] L. Qian, J. Xu, W. Sun, and Y. Peng, "Sub-aperture based blind speed side lobe (BSSL) suppression in radon Fourier transform (RFT)," in *Proc. IEEE ICSP*, Beijing, China, Oct. 2012, pp. 1880–1884.
[19] J. Zheng, H. Liu, and Q. H. Liu, "Parameterized centroid frequency-chirp rate distribution for LFM signal analysis and mechanisms of constant delay introduction," *IEEE Trans. Signal Process.*, vol. 65, no. 24, pp. 6435–6447, Dec. 2017.
[20] X. Chen, Z. Liu, and X. Wei, "Fast FRFT-based algorithm for 3-D LFM source localization with uniform circular array," *IEEE Access*, vol. 6, pp. 2130–2135, 2017.
[21] X. Cheng, A. Aubry, D. Ciuonzo, A. De Maio, and X. Wang, "Robust waveform and filter bank design of polarimetric radar," *IEEE Trans. Aerosp. Electron. Syst.*, vol. 53, no. 1, pp. 370–384, Feb. 2017.
[22] J. Xu, X.-G. Xia, S.-B. Peng, J. Yu, Y.-N. Peng, and L.-C. Qian, "Radar maneuvering target motion estimation based on generalized radon-Fourier transform," *IEEE Trans. Signal Process.*, vol. 60, no. 12, pp. 6190–6201, Dec. 2012.
[23] L. Qian, J. Xu, W. Sun, and Y. Peng, "CLEAN based blind speed side lobe (BSSL) suppression in the radon Fourier transform (RFT) for multi-target detection," in *Proc. IEEE 12th Int. Conf. Comput. Inf. Technol.*, Chengdu, China, Oct. 2012, pp. 490–495.

YONGKUN SONG was born in Henan, China, in 1993. He is currently pursuing the Ph.D. degree with the School of Electronic Science, National University of Defense Technology. He is currently a Guest Researcher with the Science and Technology on Near-Surface Detection Laboratory. His main research interests include radar signal processing, remote sensing image processing, and deep learning.

TIAN JIN was born in Hubei, China, in 1980. He received the M.S. and Ph.D. degrees from the National University of Defense Technology, China, in 2003 and 2007, respectively, where he is currently a Professor and a Ph.D. Candidate Supervisor. He is also a Guest Researcher with the Science and Technology on Near-Surface Detection Laboratory. His main research interests include hidden target radar imaging, detection and recognition, new microwave sensor mechanism and system implementation, radar, and array signal processing.

YONGPING SONG was born in Sichuan, China, in 1989. He received the M.S. and Ph.D. degrees from the National University of Defense Technology, China, in 2015 and 2019, respectively. He is currently a Teacher with Air Force Early Warning Academy. His main research interests include through-wall radar imaging, SAR image processing, and target detection and recognition.

YANSONG ZHANG was born in Heilongjiang, China, in 1992. She is currently pursuing the Ph.D. degree with the School of Electronic Science, National University of Defense Technology. Her main research interests include radar target detection and tracking, and deep learning.